

13 **Abstract:**

14 This study demonstrated the potential of seawater-driven forward osmosis for enriching organic
15 matter in digested sludge centrate. The results indicated that the cellulose triacetate membrane
16 offered better performance than the polyamide membrane in terms of organic materials
17 enrichment, fouling resistance and membrane cleaning efficiency. Membrane fouling decreased
18 the enrichment efficiency of organic matter since the deposition of suspended particulate matter
19 on the membrane surface caused fouling and loss of organic matter from the concentrated
20 sludge centrate. The results showed that increasing the draw solution concentration increased
21 flux but did not aggravate membrane fouling, however, it could reduce the efficiency of
22 physical flushing to recover the flux. Seawater showed comparable forward osmosis
23 performance to that of analytical grade NaCl as draw solutes in terms of flux and organic
24 enrichment. The results also showed that seawater as the draw solution resulted in more
25 membrane fouling and lower flux recovery compared to NaCl.

26 **Keywords:** Forward osmosis (FO); cellulose triacetate (CTA); polyamide (PA); fouling
27 behaviour; digested sludge centrate; organic matter; seawater.

28 **Water Impact Statement:**

29 Sludge centrate is a small waste stream during wastewater treatment but with a high content of
30 dissolved organic carbon and nutrients. Results from this study highlight the potential of a
31 seawater driven forward osmosis process to enrich the organic content in sludge centrate as
32 well as as key challenges for practical implementation. By enriching the organic and nutrient
33 content in sludge centrate using forward osmosis, it is possible to simultaneously reduce
34 contaminant loading and create opportunities for resource recovery.

35

36 1. Introduction

37 Forward osmosis (FO) is a robust separation platform capable of treating highly complex
38 solutions that are not suitable for conventional membrane processes ^{1, 2}. In FO, mass transfer
39 through the membrane is osmotically driven. Thus, when a draw solution (DS) is readily
40 available, the FO process can occur with very low energy input ^{1, 3-5}. The absence of external
41 hydraulic pressure can also explain the low membrane fouling tendency and excellent fouling
42 reversibility of FO. In recent years, the potential of FO to treat many complex feed solutions
43 has been demonstrated in the literature. These complex solutions include drilling and fracking
44 fluids from oil and gas exploration ⁶⁻⁹, sludge ^{10, 11}, digested sludge centrate ^{2, 12, 13}, and
45 municipal wastewater ^{4, 14, 15}.

46 A major obstacle to full scale deployment of FO is the lack of a suitable DS ¹. Issues associated
47 with cost of the draw solutes, regeneration, and loss of draw solutes due to reverse diffusion
48 can increase the operating cost, thereby hindering the feasibility of FO applications ^{1, 16, 17}. In
49 this context, seawater, which is abundant and cheaply available in coastal areas, has been
50 increasingly considered as a potential DS ^{1, 16}. The diluted seawater released from the process
51 can be returned to the sea, and thus, DS regeneration is not necessary.

52 In a typical wastewater treatment plant, the sludge is anaerobically digested. The digested
53 sludge is then dewatered to obtain biosolids for land application. The liquid from this
54 dewatering process is called sludge centrate, which has a high content of suspended solids,
55 nutrients, and organic matter ¹³. Due to the difficulties associated with the treatment of this
56 sludge centrate, in most cases, it is returned to the headworks of the treatment plant. The
57 recirculation of untreated sludge centrate to the headworks leads to additional organic and
58 nutrient loading, and deprive the plant from any opportunities for energy and nutrient recovery
59 ^{12, 18}.

60 The use of FO to pre-concentrate sludge centrate has been investigated in several recent studies
61 ^{2, 13}. However, draw solutes such as MgCl₂ and NaCl are expensive and must be regenerated.
62 On the other hand, seawater appears to be a particularly promising DS for pre-concentrating
63 sludge centrate. Ansari et al. ¹² has recently demonstrated a seawater-driven FO process for
64 phosphorus recovery from digested sludge centrate with a specific focus on evaluating the
65 efficiency of nutrient recovery. [Results from previous studies suggest that identifying the most
66 suitable membrane type and orientation is necessary to ensure the best performance of seawater-
67 driven FO process for pre-concentrating sludge centrate ^{2, 10-12}. More importantly,
68 understanding of the fouling process and developing strategies to control fouling need to be
69 discussed to guarantee the long-term operation of the FO system. It is also necessary to consider
70 all other factors affecting water flux and membrane fouling, such as membrane pre-wetting and
71 draw solution.](#)

72 This study aims to elucidate the effects of membrane materials, prewetting procedures and DS
73 on the performance of seawater-driven forward osmosis for pre-concentrating organic matter

74 in the sludge centrate. The performance of the FO process is observed in terms of chemical
75 oxygen demand (COD) enrichment, membrane fouling and flux recovery by physical cleaning.
76 Comparison between seawater and analytical grade NaCl as the DS was made to highlight the
77 potential and challenges of using seawater for enriching COD in sludge centrate.

78 **2. Materials and methods**

79 **2.1. Forward osmosis system and membranes**

80 A lab-scale cross-flow FO system (Figure 1) was used. The FO system included a membrane
81 cell, two variable speed gear pumps (Micropump, Vancouver, Washington, USA), conductivity
82 and temperature controllers, and a digital balance to measure the flux. The FO membrane cell
83 consisted of two symmetric rectangular chambers for the feed and draw solutions, respectively.
84 The internal dimensions of each chamber were 10 cm in length, 5 cm in width and 0.2 cm in
85 height. The system was operated in the counter-current mode. The FO membranes were
86 positioned either in active layer facing feed solution (AL-FS) orientation, or active layer facing
87 draw solution (AL-DS) orientation.

88 Flat sheet FO membranes were obtained from Hydration Technology Innovations (HTI,
89 Albany, OR) and Porifera, Inc. (Hayward, California, USA). The HTI membrane had an
90 asymmetric structure and was made of cellulose triacetate (CTA) with an embedded polyester
91 mesh for mechanical support. The Porifera membrane was a thin film composite (TFC)
92 membrane consisting of a thin polyamide (PA) layer on a microporous polysulfone supporting
93 layer. Key properties of the HTI and Porifera membranes were summarised in Table 1.

94 **Table 1:** Key properties of the active layer of the FO membranes ^{19, 20}.

Membrane	HTI-CTA	Porifera-PA
Water permeability (A) (L/m ² .h.bar)	0.84	3.2
Salt (NaCl) permeability (B) (L/m ² .h)	0.32	0.41
Structural parameter (S) (mm)	0.57	0.46
Contact angle (°)	61	49.5
Surface roughness (nm)	3.8	57.4
Zeta potential at pH = 7 (mV)	-5	-16

95

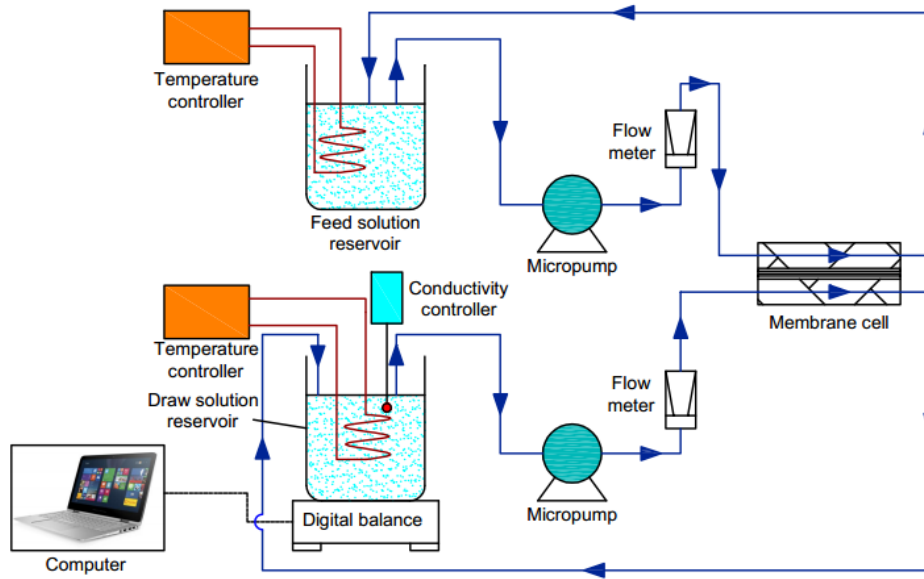


Figure 1: Schematic diagram of the lab-scale FO system.

2.2. Feed solution and draw solution

In this study, seawater and NaCl solutions were used as DSs. Seawater was collected from North Wollongong Beach (Wollongong, New South Wales, Australia) and was filtered using filter paper with a pore size of 1 μm prior to the experiments. NaCl solutions of 0.25, 0.5, 0.75 and 1 M were prepared using analytical grade NaCl and deionised (DI) water. Anaerobically digested sludge centrate was collected from a high-speed centrifuge at the Shellharbour Wastewater Treatment Plant (Shellharbour, New South Wales, Australia). The centrate was pre-filtered using a 0.2 mm plastic screen to remove any large objects. The compositions of seawater and digested sludge centrate were summarised in Table 2.

Table 2. Composition of seawater and digested sludge centrate (values indicated average \pm standard deviation of at least three samples).

Parameters	Unit	Seawater	Digested sludge centrate
pH	-	7.3 ± 0.2	7.1 ± 0.1
Electrical conductivity	mS/cm	44.2 ± 0.3	6.8 ± 0.1
Osmotic pressure	bar	28.1 ± 0.6	6.5 ± 0.1
Total solids	g/L	31.7 ± 2.8	1.6 ± 0.1
COD	mg/L	-	420.3 ± 15.5
Ammonia	mg/L	-	520 ± 2.6
Total phosphorus (as PO_4^{3-})	mg/L	-	371.5 ± 1.4

109 2.3. Membrane prewetting

110 Prewetting was conducted by soaking in a solution containing 70% ethanol and 30% water for
111 45 min. Following soaking, the membrane was rinsed and preserved in DI water overnight prior
112 to filtration experiments.

113 2.4. Experimental protocols

114 All FO experiments were conducted in four steps. In the first step, DI water was used as the
115 feed solution (FS) for 30 min to determine the pure water flux. In the second step, DI water was
116 substituted with sludge centrate and the FO experiment was conducted until a water recovery
117 of 55% had been achieved. Duration of this second step varied from experiment to experiment
118 ranging from 24 to 120 hours. At specified time intervals, 10 mL samples were collected from
119 the feed for analysis. In the third step, the draw and feed solutions were replaced by DI water
120 to facilitate membrane cleaning by flushing at a cross-flow velocity of 24 cm/s for 20 min. In
121 the last step, the pure water flux was determined again using DI water under identical
122 experimental conditions as in the first step. In all experiments, initial volumes of the feed and
123 draw solutions were 1 and 3 L, respectively. The circulation flow rate of the feed and the draw
124 solution was 0.8 L/min (i.e., cross flow velocity of 13 cm/s).

125 2.5. Calculations

126 Water flux (J_w) was calculated based on the change in weight of DS, and expressed as in Eq.
127 (1):

$$128 \quad J_w = \frac{m_{t_i} - m_{t_{i-1}}}{(t_i - t_{i-1}) \times \rho \times A_m} = \frac{\Delta m_i}{\Delta t_i \times \rho \times A_m} \quad (\text{Eq. 1})$$

129 Where: Δm_i : the change in weight of DS over a time interval (g)

130 Δt_i : a time interval (h)

131 ρ : the solution density (g/cm^3)

132 A_m : the effective membrane area (m^2)

133 Water recovery was determined based on the ratio of the cumulative permeate volume and the
134 initial volume of FS, and presented as in Eq. (2):

$$135 \quad \text{Water recovery (\%)} = \frac{\int_0^t A_m \times J_w \times dt}{V_{\text{initial}}} \times 100\% \quad (\text{Eq. 2})$$

136 Where: J_w : the observed water flux at time t

137 V_{initial} : the initial volume of FS

138

139

140 The draw solute flux (J_s) was calculated by Eq. (3):

$$141 \quad J_s = \frac{C_{f,t_2} \times V_{f2} - C_{f,t_1} \times V_{f1}}{\Delta t \times A_m} \quad (\text{Eq. 3})$$

142 Where: C_{f,t_2} : The concentration of draw solute in FS at time t_2 (g/L)

143 V_{f2} : The volume of FS at time t_2 (L)

144 C_{f,t_1} : The concentration of draw solute in FS at time t_1 (g/L)

145 V_{f1} : The volume of FS at time t_1 (L)

146 Δt : a certain period of filtration time (h)

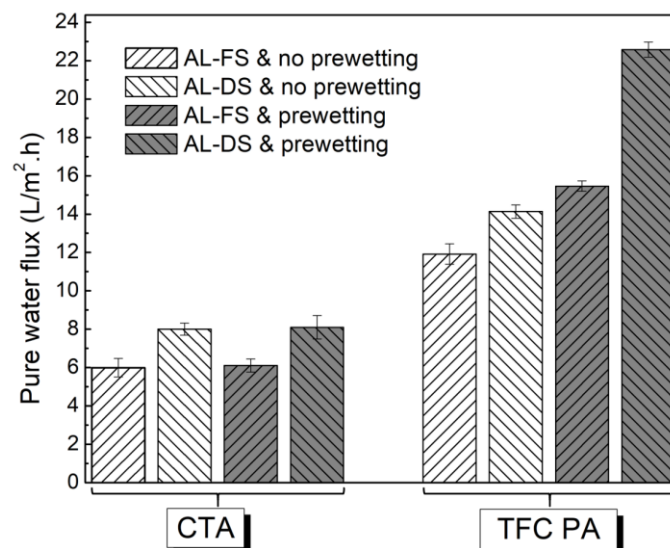
147 2.6. Analytical methods

148 Key water quality parameters of digested sludge centrate and seawater were measured
149 according to standard methods. COD was determined using a Hach DRB200 COD Reactor and
150 Hach DR3900 spectrophotometer following the US-EPA Standard Method 5220. Temperature
151 and pH of solutions were measured by an Orion 4-Star Plus pH/conductivity meter (Thermo
152 Scientific, Waltham, MA).

153 The surface characteristics of the FO membranes were characterized using scanning electron
154 microscopy (SEM) (JOEL, JSM-6400LV, Japan). Prior to taking SEM images, coupon
155 membrane samples were coated with a thin layer of gold.

156 3. Results and discussions

157 3.1. Pure water flux under different conditions



158

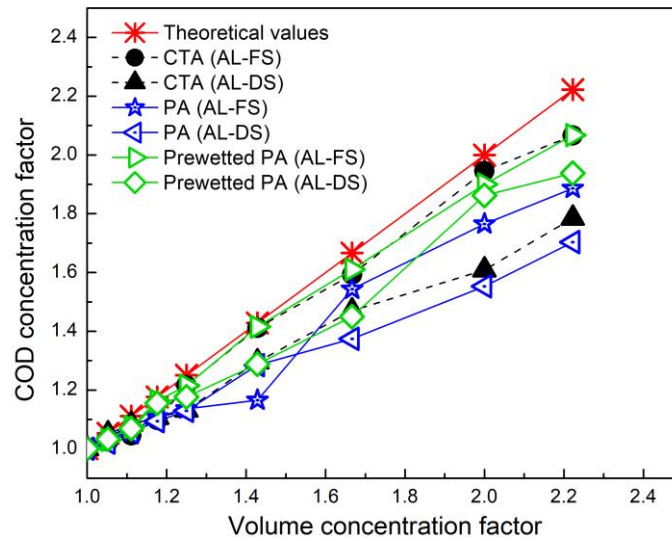
159 **Figure 2:** Pure water fluxes of CTA and PA FO membranes using seawater as DS in AL-FS
160 and AL-DS orientations with and without prewetting.

161 Under the same experimental conditions, the TFC PA membrane showed a higher pure water
162 flux than that of the CTA membrane (Figure 2). This observation could be explained by the A
163 value (water permeability under a hydraulic pressure) and the structure parameter (S value) of
164 these two membranes (Table 1). Indeed, the A value of the TFC PA membrane was
165 approximately 4 times higher than that of the CTA membrane. The structural parameter value
166 of the TFC PA membrane (460 μm) was slightly lower than that of the CTA membrane (570
167 μm)¹⁹. Previous studies have demonstrated that a smaller structural parameter results in less
168 severe internal concentration polarization (ICP) and, thus, higher water flux^{1,19}. It is noteworthy
169 that in the FO process, concentration polarisation could also influence the water flux. Thus, the
170 difference in pure water flux between the TFC PA and CTA membranes was not necessarily
171 proportional to the difference in their A and S values.

172 The AL-DS orientation exhibited a higher pure water flux compared to the AL-FS orientation.
173 The difference in water flux between these two orientations was considerably less than the
174 comparison between the TFC PA and CTA membranes discussed above. Indeed, the higher
175 water flux under the AL-DS orientation compared to the AL-FS orientation could be solely
176 attributed to a less severe ICP condition^{1, 21, 22}.

177 Prewetting significantly improved the pure water flux of the TFC PA membrane but had a
178 negligible impact on the CTA membrane. As a result of prewetting, water flux of the PA
179 membrane increased by 29.7% and 59.7% under the AL-FS and AL-DS orientation,
180 respectively (Figure 2). There were two possible reasons for this notable increase in flux by the
181 TFC PA membrane after prewetting, namely swelling of the PA skin layer and prewetting of
182 the polysulfone supporting layer. The PA skin layer could swell in alcohol causing an increase
183 in the effective pore size and thus, increased the water flux²⁰. However, there was no discernible
184 increase in the reverse salt flux due to prewetting (data not shown). Thus, swelling was not
185 expected to be a major reason for the improvement in water flux observed here. The polysulfone
186 supporting layer was hydrophobic and could not be completely wetted by water²³. Compared
187 to water, ethanol had a lower surface tension, thus, could easily penetrate into the porous
188 structure and prewet the pores of the polysulfone supporting layer for subsequent water
189 permeation^{23, 24}. Conversely, CTA membrane was asymmetric and CTA material was readily
190 hydrophilic. Thus, prewetting did not affect its pure water flux (Figure 2)²⁵.

191 **3.2. Pre-concentration of digested sludge centrate by FO**

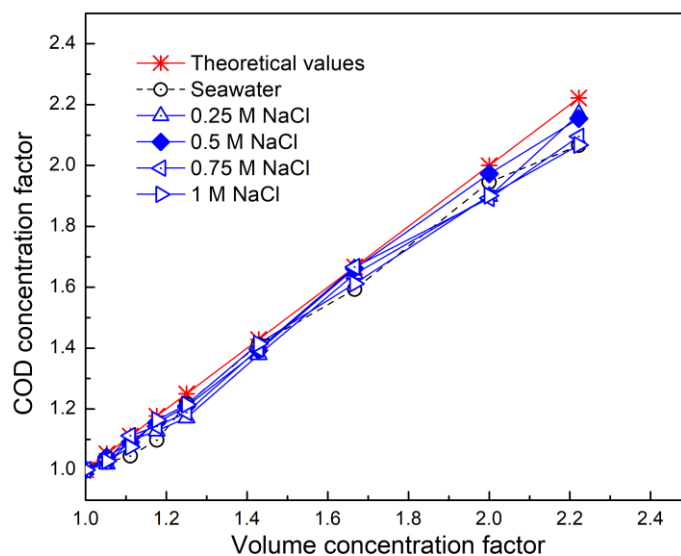


192

193 **Figure 3:** The performance of FO for enrichment of COD in digested sludge centrate using
 194 seawater as the DS. The theoretical COD concentration factor was calculated assuming 100%
 195 COD retention by the FO membrane.

196 As the sludge centrate was concentrated by FO, COD concentration increased proportionally
 197 (Figure 3). In all cases, the COD concentration factor was lower than the theoretical value
 198 assuming complete COD retention. The observed difference between the COD concentration
 199 factor and theoretical value could possibly be attributed to the deposition of particulate COD
 200 materials on the membrane surface. In fact, there was a correlation between membrane fouling
 201 and the COD enrichment results in Figure 3 as discussed further in section 3.3.

202 The best performance in terms of COD enrichment was from the CTA membrane with the AL-
 203 FS orientation (Figure 3). The active layer of the CTA membrane had a lower surface roughness
 204 than its own supporting layer as well as that of the TFC PA membrane^{20, 26-28}. Thus, due to the
 205 hydrodynamic drag force from the cross flow, the deposition of organic substances on the CTA
 206 membrane was expected to be less compared to the TFC PA membrane. **In addition, surface**
 207 **chemistry interaction between organic matter and the membrane surface could be a reason for**
 208 **the lower organic enrichment when using the PA membrane.** The PA membrane has a
 209 considerable number of highly polar carboxylic functional groups on its surface and has
 210 significant affinity towards organic colloids in the FS²⁰. As a result, the accumulation of
 211 organic matter on the PA membrane surface could be enhanced, thus reducing COD
 212 concentration in the bulk feed. It is noted that this combination (CTA under AL-FS orientation)
 213 also had the lowest initial water flux. However, it appears that water flux did not affect COD
 214 enrichment performance as demonstrated below.



215

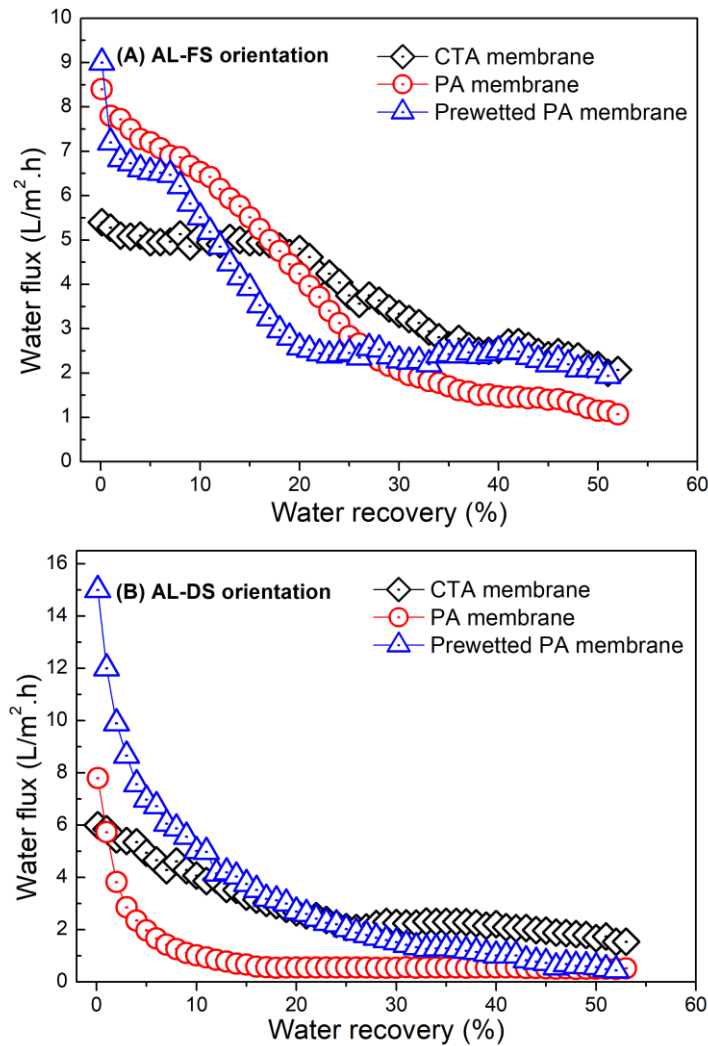
216 **Figure 4:** The performance of FO for enrichment of COD in digested sludge centrate using
 217 the NaCl solution as the DS and the CTA membrane in the AL-FS orientation. Note: The
 218 theoretical COD concentration factor was calculated assuming 100% COD retention by the
 219 FO membrane.

220 DS concentration did not affect the enrichment of COD by FO (Figure 4). No significant
 221 difference in COD enrichment was observed when the NaCl DS concentration increased from
 222 0.25 to 1 M (Figure 4). The initial water flux was proportional to the DS concentration. Thus,
 223 results in Figure 4 also suggested that water flux did not affect COD enrichment as discussed
 224 above.

225 Seawater showed comparable COD enrichment performance to that of analytical grade NaCl
 226 as the draw solutes. The osmotic potential of seawater was similar to that of the 0.5 M NaCl
 227 solution^{29, 30}. Seawater was readily available in coastal areas and thus it was a low-cost DS.
 228 However, in addition to NaCl, seawater contained many other salts. Some of them were
 229 sparingly soluble and might cause membrane scaling as further discussed in section 3.3.2.

230 **3.3. Factors affecting fouling behaviour**

231 *3.3.1. Membrane properties and orientations*



232

233 **Figure 5:** Fouling behaviour of the FO membranes in (A) AL-FS orientation and (B) AL-DS
234 orientation using seawater as DS.

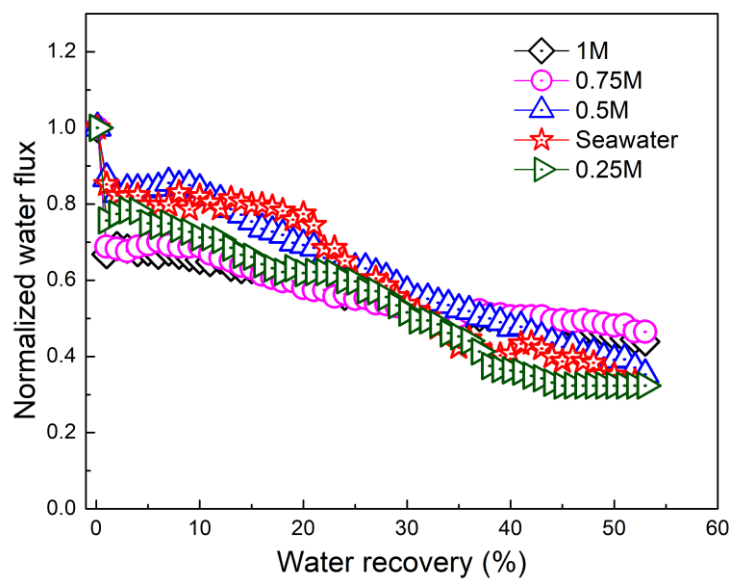
235 In all cases, membrane fouling was significant as indicated by significant water flux decline
236 during COD enrichment (Figure 5). The decrease in water flux could be mostly attributed to
237 the formation of a cake layer on the membrane surface. This cake layer caused an additional
238 hydraulic resistance and increased concentration polarisation, thus reducing water flux.

239 In good agreement to the data in Figure 3, the CTA membrane was less susceptible to fouling
240 than the TFC PA membrane regardless of the membrane orientation. As described above, this
241 result was likely due to the smooth surface of the CTA membrane. The higher roughness and
242 prominent ridge-and-valley structure of the PA membrane surface could exacerbate the
243 deposition of foulants, thus more severe fouling²⁰. Additionally, a high density of carboxylic
244 functional groups in the structure of the PA membrane could be potentially vulnerable to fouling

245 ³¹. In the presence of Ca²⁺ ions, carboxyl acid functional groups could lead to bridging of
246 membrane surface and Ca²⁺-organic foulants, thus probably exacerbating organic fouling.

247 The AL-FS orientation showed less fouling than the AL-DS orientation. There were several
248 possible explanations. As mentioned above, the lower roughness of the active layer in the AL-
249 FS orientation could alleviate the accumulation of foulants on the membrane surface. FO
250 operation under the AL-DS orientation was susceptible to internal clogging since organic
251 molecules could readily penetrate the porous supporting layer. In addition, the high reverse
252 solute diffusion in the AL-DS orientation could increase the osmotic potential of the feed,
253 decreased effective driving force, and thus, reduced the water flux ²¹.

254 3.3.2. Draw solution



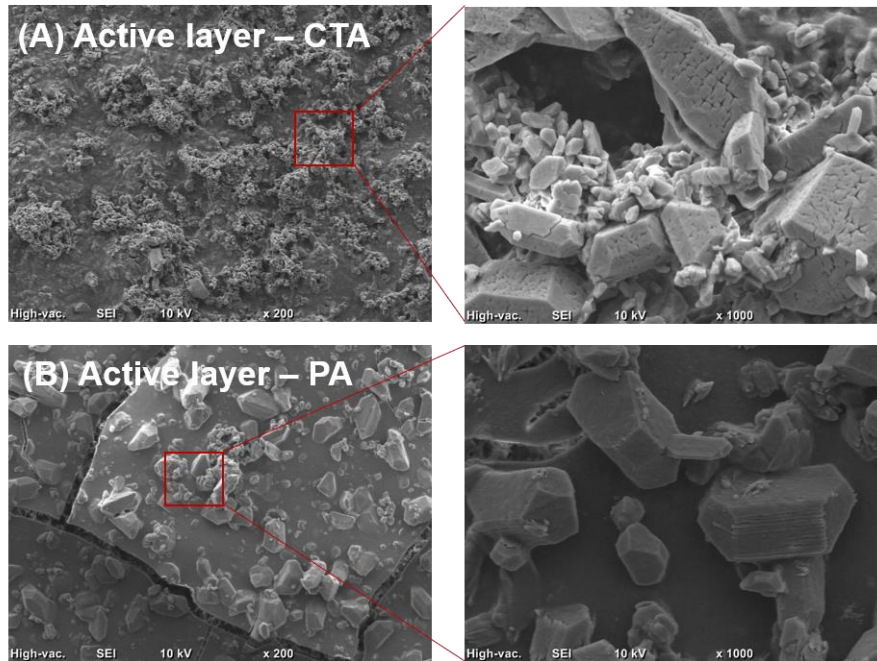
255

256 **Figure 6:** Comparison of fouling behaviour towards CTA membranes in the AL-FS
257 orientation using seawater and the NaCl solutions at different concentration as DSs.

258 As discussed in section 3.2, the CTA membrane under the AL-FS orientation demonstrated the
259 best suitability for enriching organic matter in concentrate. Thus, the CTA membrane under the
260 AL-FS orientation was used for further investigation. Increasing the DS concentration led to a
261 higher initial water flux (Figure 9), but no significant impacts on membrane fouling (Figure 6).
262 The elevated initial water flux was a result of the increased driving force of water transport due
263 to an increase in the concentration gradient along the membrane. However, the extent of fouling
264 in all cases was nearly the same. This was probably because of the smoothness of the CTA
265 membrane surface that could effectively minimize the accumulation and deposition of foulants.
266 In addition, this could be explained using the theory of ‘critical DS concentration’. According
267 to this concept, fouling could be less severe at below the critical DS concentration ^{32, 33}. It is
268 possible that the used DS concentrations in this study were lower than the critical DS
269 concentration, thus, the impacts of DS concentration on fouling were insignificant.

270 Seawater exhibited similar fouling to that from the 0.5 M NaCl solution as the DSs. This
271 observation was consistent with the data shown in Figure 4, and thus could also be explained
272 by the same reason as referred to earlier. However, it is noted that the flux profile when using
273 seawater was less stable than that of using the 0.5 M NaCl solution. Multivalent ions in
274 seawater, such as Ca^{2+} , Mg^{2+} , SO_4^{2-} and PO_4^{3-} could act as fouling promoters, and scaling
275 precursors through the reverse solute diffusion, thus increasing fouling potential.

276 *3.3.3. Fouling layer characteristics*

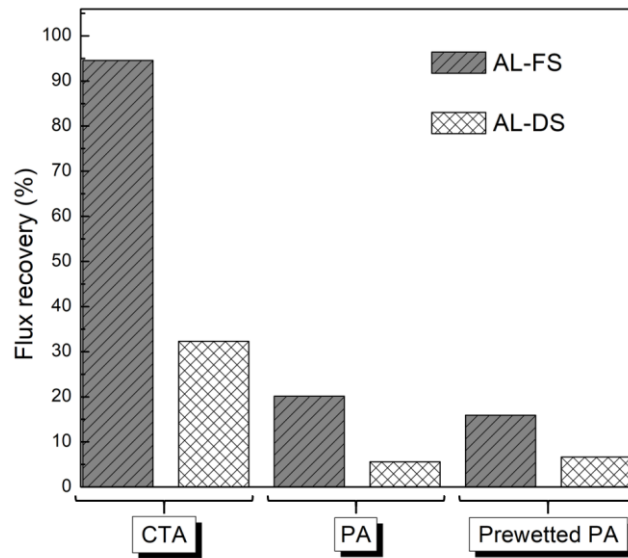


277
278 **Figure 7:** SEM images of the active layer of (A) the fouled CTA membrane and (B) the
279 fouled TFC PA membrane in the AL-FS orientation using seawater DS.

280 A notable contrast in the morphology of the fouling layer on the CTA and TFC PA membranes
281 could be observed (Figure 7). The fouling layer on the active layer surface of the CTA
282 membrane was loose and soft (Figure 7A) while that of the PA membrane was dense and firm
283 (Figure 7B). The observed irregular shape and size of crystals and organic cake-layer on the
284 membrane surface suggested the presence of both organic and inorganic foulants.

285
286
287
288
289
290

291 **3.4. Cleaning and flux reversibility**



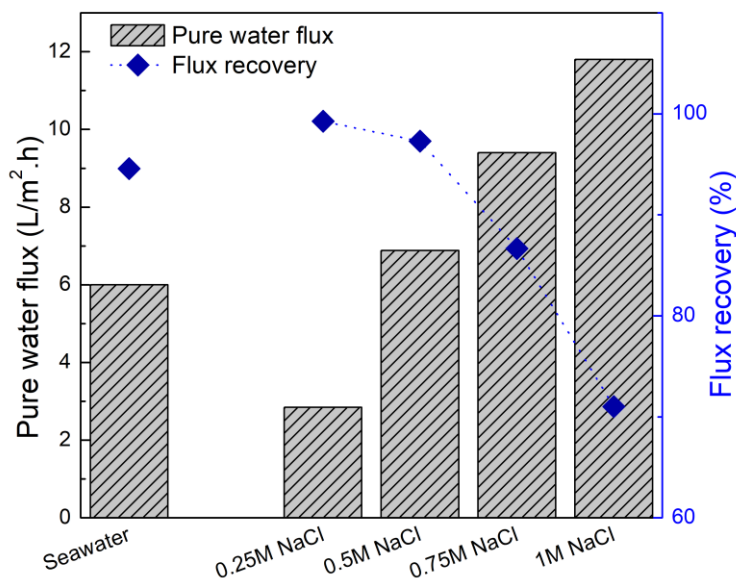
292

293 **Figure 8:** Flux recovery of the fouled CTA, PA and prewetted PA membranes using seawater
294 DS after physical flushing.

295 As expected, flux recovery by flushing in the AL-FS orientation was higher than that in the AL-
296 DS orientation (Figure 8). Flux recovery was proportional to the efficiency of foulant removal
297 from the membrane surface. In the AL-FS orientation, the deposition of foulants on the
298 membrane was a surface phenomenon and the fouling cake could be readily removed by shear
299 force from flushing. On the other hand, in the AL-DS orientation, the feed solution was in
300 contact with the supporting layer and due to pore clogging of the supporting layer, flux
301 recoverability was much lower than in the AL-FS orientation (Figure 8).

302 The highest flux recovery (95%) was observed with the CTA membrane in the AL-FS
303 orientation (Figure 8). Together with the high COD enrichment performance shown in Figure
304 3, this result suggested that the CTA membrane in the AL-FS orientation was the most suitable
305 for sludge centrate. This result was also consistent with the loose and soft fouling layer of the
306 CTA membrane under the AL-FS orientation previously shown in Figure 7A.

307 Flushing was not efficient in restoring the water flux of the PA and prewetted PA membranes.
308 There were two possible reasons. Firstly, foulants deposited on a rough surface of the PA
309 membrane could be sheltered from cross-flow shear force, thus decreasing the number of
310 foulants detached from the membrane surface. Secondly, the highly polar carboxylic functional
311 groups on the PA membrane surface were available for ionic bonding with foulants, thus
312 improving foulant adhesion²⁰. In contrast, the CTA membrane was only slightly negatively
313 charged and did not have free carboxyl functional groups that could interact with the foulants
314²⁰.

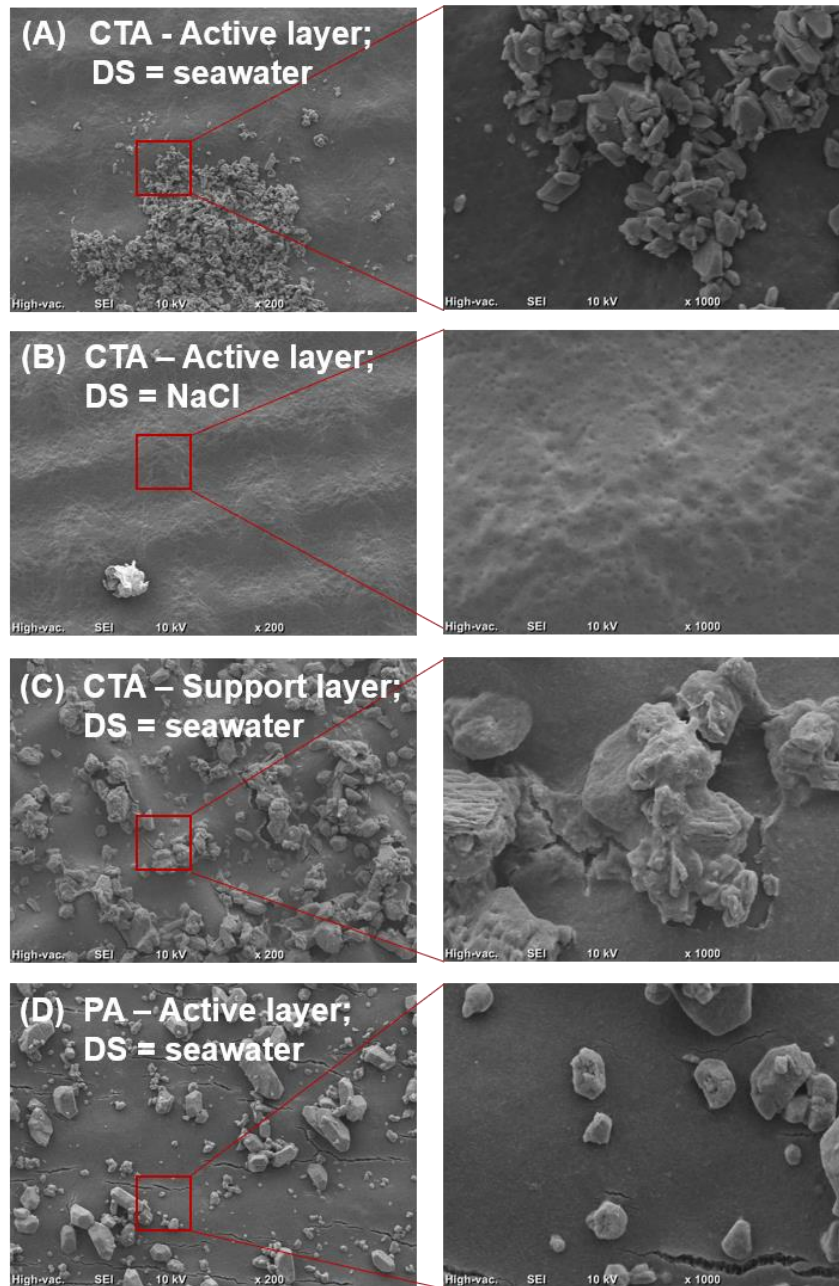


315

316 **Figure 9:** Comparison of pure water fluxes and flux recovery of CTA membranes in the AL-
 317 FS orientation using seawater and NaCl DS.

318 Increasing the DS concentration resulted in a higher pure water flux but also reduced flux
 319 recovery by flushing (Figure 9). Indeed, as the NaCl concentration increased from 0.25 to 1 M,
 320 flux recovery decreased from nearly 100% to 70%. Since the DS concentration was proportional
 321 to water flux, results in Figure 9 showed that the extent of irreversible fouling (by flushing) was
 322 inversely correlated to the initial flux. A denser and more compact fouling was formed at higher
 323 initial flux, thereby, impairing the efficiency of flushing.

324 Seawater had a similar osmotic potential to a 0.5 M NaCl solution. However, a slightly lower
 325 flux recovery was observed when using seawater as the DS compared to the 0.5 M NaCl
 326 solution. The complex composition of seawater could result in a less reversible fouling layer.
 327 Indeed, multivalent cations (such as Ca²⁺ and Mg²⁺) in seawater could exacerbate fouling and
 328 render fouling layer more adhesive, thus lowering the flux recoverability by flushing.



329

330 **Figure 10:** SEM images of (A) the active layer of the cleaned CTA membrane in the AL-FS
 331 orientation using seawater as DS, (B) the active layer of the cleaned CTA membrane in the
 332 AL-FS orientation using the 0.5 M NaCl solution as DS, (C) the supporting layer of the
 333 cleaned CTA membrane in the AL-DS orientation using seawater as DS and (D) the active
 334 layer of the cleaned PA membrane in the AL-FS orientation using seawater DS.

335 The complex composition of seawater and the membrane characteristics were observed to
 336 govern the cleaning efficiency of flushing (Figure 10). After flushing, the CTA membrane
 337 active surface in the AL-FS orientation (seawater as DS) still had some salt crystals and organic
 338 particles (Figure 10A). In contrast, when using the 0.5 M NaCl solution, the membrane was
 339 mostly clean after flushing (Figure 10B). This was consistent with the data in Figure 9 that
 340 indicated how the complex composition of seawater resulted in a more adhesive fouling layer.

341 In addition, SEM images indicated that both for CTA membrane under the AL-DS orientation
342 (Figure 10C) and PA membrane in the AL-FS orientation (Figure 10D) flushing removed
343 crystals significantly, but the organic layers only partly. These observations resulted from
344 synergistic effects of membrane roughness and chemical structure of these membranes on
345 fouling as discussed above.

346 **4. Conclusions**

347 Results from this study demonstrated the potential of the FO process to enrich COD in sludge
348 centrate. Compared to the TFC PA membrane, the CTA membrane in the AL-FS orientation
349 showed a much better COD enrichment efficiency, lower fouling, and higher flux recovery by
350 simple flushing. There was a correlation between membrane fouling and COD enrichment
351 efficiency. In other words, COD enrichment efficiency decreased when organic matter
352 accumulated on the membrane surface, causing fouling. [The results also showed that membrane
353 fouling was not affected by the DS concentration \(or initial water flux\) possibly because of the
354 low initial flux in this study](#), however, flux recovery by membrane flushing decreased as the
355 initial water flux increased. Seawater is a potentially low-cost and effective DS for COD
356 enrichment. However, compared to NaCl, seawater as the DS led to more severe membrane
357 fouling and lower flux recovery by flushing. [Further research is necessary to address the issue
358 of membrane fouling when using seawater as the DS for COD enrichment in sludge centrate.](#)

359 **Acknowledgments**

360 Scholarship support to Minh T. Vu by the University of Wollongong is gratefully
361 acknowledged. Authors would like to thank the Shellharbour Wastewater Treatment Plant for
362 their assistance with the collection of digested sludge centrate.

363 **References**

- 364 1. K. Luttmiah, A. R. Verliefde, K. Roest, L. C. Rietveld and E. R. Cornelissen, Forward
365 osmosis for application in wastewater treatment: a review, *Water Res*, 2014, **58**, 179-
366 197.
- 367 2. M. Xie, L. D. Nghiem, W. E. Price and M. Elimelech, Toward Resource Recovery from
368 Wastewater: Extraction of Phosphorus from Digested Sludge Using a Hybrid Forward
369 Osmosis–Membrane Distillation Process, *Environmental Science & Technology*
370 *Letters*, 2014, **1**, 191-195.
- 371 3. A. A. Alturki, J. A. McDonald, S. J. Khan, W. E. Price, L. D. Nghiem and M. Elimelech,
372 Removal of trace organic contaminants by the forward osmosis process, *Separation and*
373 *Purification Technology*, 2013, **103**, 258-266.
- 374 4. A. J. Ansari, F. I. Hai, W. Guo, H. H. Ngo, W. E. Price and L. D. Nghiem, Factors
375 governing the pre-concentration of wastewater using forward osmosis for subsequent
376 resource recovery, *Sci Total Environ*, 2016, **566-567**, 559-566.
- 377 5. T. Cath, A. Childress and M. Elimelech, Forward osmosis: Principles, applications, and
378 recent developments, *Journal of Membrane Science*, 2006, **281**, 70-87.

- 379 6. G. Chen, Z. Wang, L. D. Nghiem, X.-M. Li, M. Xie, B. Zhao, M. Zhang, J. Song and
380 T. He, Treatment of shale gas drilling flowback fluids (SGDFs) by forward osmosis:
381 Membrane fouling and mitigation, *Desalination*, 2015, **366**, 113-120.
- 382 7. Y. Chun, S.-J. Kim, G. J. Millar, D. Mulcahy, I. S. Kim and L. Zou, Forward osmosis
383 as a pre-treatment for treating coal seam gas associated water: Flux and fouling
384 behaviour, *Desalination*, 2017, **403**, 144-152.
- 385 8. B. D. Coday, P. Xu, E. G. Beaudry, J. Herron, K. Lampi, N. T. Hancock and T. Y. Cath,
386 The sweet spot of forward osmosis: Treatment of produced water, drilling wastewater,
387 and other complex and difficult liquid streams, *Desalination*, 2014, **333**, 23-35.
- 388 9. X.-M. Li, B. Zhao, Z. Wang, M. Xie, J. Song, L. D. Nghiem, T. He, C. Yang, C. Li and
389 G. Chen, Water reclamation from shale gas drilling flow-back fluid using a novel
390 forward osmosis–vacuum membrane distillation hybrid system, *Water Science and
391 Technology*, 2014, **69**, 1036.
- 392 10. S. Liyanaarachchi, V. Jegatheesan, I. Obagbemi, S. Muthukumaran and L. Shu, Effect
393 of feed temperature and membrane orientation on pre-treatment sludge volume
394 reduction through forward osmosis, *Desalination and Water Treatment*, 2015, **54**, 838-
395 844.
- 396 11. N. C. Nguyen, H. T. Nguyen, S.-S. Chen, N. T. Nguyen and C.-W. Li, Application of
397 forward osmosis (FO) under ultrasonication on sludge thickening of waste activated
398 sludge, *Water Science and Technology*, 2015, **72**, 1301.
- 399 12. A. J. Ansari, F. I. Hai, W. E. Price and L. D. Nghiem, Phosphorus recovery from
400 digested sludge centrate using seawater-driven forward osmosis, *Separation and
401 Purification Technology*, 2016, **163**, 1-7.
- 402 13. R. W. Holloway, A. E. Childress, K. E. Dennett and T. Y. Cath, Forward osmosis for
403 concentration of anaerobic digester centrate, *Water Res*, 2007, **41**, 4005-4014.
- 404 14. Z. Wang, J. Zheng, J. Tang, X. Wang and Z. Wu, A pilot-scale forward osmosis
405 membrane system for concentrating low-strength municipal wastewater: performance
406 and implications, *Scientific Reports*, 2016, **6**, 21653.
- 407 15. W. Xue, T. Tobino, F. Nakajima and K. Yamamoto, Seawater-driven forward osmosis
408 for enriching nitrogen and phosphorous in treated municipal wastewater: effect of
409 membrane properties and feed solution chemistry, *Water Res*, 2015, **69**, 120-130.
- 410 16. Q. Ge, M. Ling and T.-S. Chung, Draw solutions for forward osmosis processes:
411 Developments, challenges, and prospects for the future, *Journal of Membrane Science*,
412 2013, **442**, 225-237.
- 413 17. D. L. Shaffer, J. R. Werber, H. Jaramillo, S. Lin and M. Elimelech, Forward osmosis:
414 Where are we now?, *Desalination*, 2015, **356**, 271-284.
- 415 18. W. Mo and Q. Zhang, Energy–nutrients–water nexus: Integrated resource recovery in
416 municipal wastewater treatment plants, *Journal of Environmental Management*, 2013,
417 **127**, 255-267.
- 418 19. W. Luo, M. Xie, F. I. Hai, W. E. Price and L. D. Nghiem, Biodegradation of cellulose
419 triacetate and polyamide forward osmosis membranes in an activated sludge bioreactor:
420 Observations and implications, *Journal of Membrane Science*, 2016, **510**, 284-292.
- 421 20. N. M. Mazlan, P. Marchetti, H. A. Maples, B. Gu, S. Karan, A. Bismarck and A. G.
422 Livingston, Organic fouling behaviour of structurally and chemically different forward

- 423 osmosis membranes – A study of cellulose triacetate and thin film composite
424 membranes, *Journal of Membrane Science*, 2016, **520**, 247-261.
- 425 21. M. Xie, W. E. Price and L. D. Nghiem, Rejection of pharmaceutically active compounds
426 by forward osmosis: Role of solution pH and membrane orientation, *Separation and*
427 *Purification Technology*, 2012, **93**, 107-114.
- 428 22. S. Zhao, L. Zou and D. Mulcahy, Effects of membrane orientation on process
429 performance in forward osmosis applications, *Journal of Membrane Science*, 2011, **382**,
430 308-315.
- 431 23. J. Kochan, T. Wintgens, R. Hochstrat and T. Melin, Impact of wetting agents on the
432 filtration performance of polymeric ultrafiltration membranes, *Desalination*, 2009, **241**,
433 34-42.
- 434 24. J. R. McCutcheon and M. Elimelech, Influence of membrane support layer
435 hydrophobicity on water flux in osmotically driven membrane processes, *Journal of*
436 *Membrane Science*, 2008, **318**, 458-466.
- 437 25. T. Y. Cath, M. Elimelech, J. R. McCutcheon, R. L. McGinnis, A. Achilli, D. Anastasio,
438 A. R. Brady, A. E. Childress, I. V. Farr, N. T. Hancock, J. Lampi, L. D. Nghiem, M.
439 Xie and N. Y. Yip, Standard Methodology for Evaluating Membrane Performance in
440 Osmotically Driven Membrane Processes, *Desalination*, 2013, **312**, 31-38.
- 441 26. M. Elimelech, Z. Xiaohua, A. E. Childress and H. Seungkwan, Role of membrane
442 surface morphology in colloidal fouling of cellulose acetate and composite aromatic
443 polyamide reverse osmosis membranes, *Journal of Membrane Science*, 1997, **127**, 101-
444 109.
- 445 27. E. M. V. Hoek, S. Bhattacharjee and M. Elimelech, Effect of Membrane Surface
446 Roughness on Colloid–Membrane DLVO Interactions, *Langmuir*, 2003, **19**, 4836-
447 4847.
- 448 28. Q. She, R. Wang, A. G. Fane and C. Y. Tang, Membrane fouling in osmotically driven
449 membrane processes: A review, *Journal of Membrane Science*, 2016, **499**, 201-233.
- 450 29. A. Poisson and A. Papaud, Diffusion coefficients of major ions in seawater, *Marine*
451 *Chemistry*, 1983, **13**, 265-280.
- 452 30. L. Yuan-Hui and S. Gregory, Diffusion of ions in sea water and in deep-sea sediments,
453 *Geochimica et Cosmochimica Acta*, 1974, **38**, 703-714.
- 454 31. M. Xie and S. R. Gray, Gypsum scaling in forward osmosis: Role of membrane surface
455 chemistry, *Journal of Membrane Science*, 2016, **513**, 250-259.
- 456 32. Q. She, Y. K. W. Wong, S. Zhao and C. Y. Tang, Organic fouling in pressure retarded
457 osmosis: Experiments, mechanisms and implications, *Journal of Membrane Science*,
458 2013, **428**, 181-189.
- 459 33. S. Zou, Y.-N. Wang, F. Wicaksana, T. Aung, P. C. Y. Wong, A. G. Fane and C. Y.
460 Tang, Direct microscopic observation of forward osmosis membrane fouling by
461 microalgae: Critical flux and the role of operational conditions, *Journal of Membrane*
462 *Science*, 2013, **436**, 174-185.
- 463